*Superlattices and Microstructures, Vol. 27, No. 5/6, 2000*
doi:10.1006/spmi.2000.0867
Available online at http://www.idealibrary.com on IDEAL

# Effect of boundaries and impurities on electron–phonon dephasing

A. SERGEEV, V. MITIN
*Department of ECE, Wayne State University, Detroit, MI 48202, U.S.A.*

*(Received 28 February 2000)*

Electron scattering from boundaries and impurities destroys the single-particle picture of the electron–phonon interaction. We show that quantum interference between 'pure' electron–phonon and electron–boundary/impurity scattering may result in the reduction as well as to the significant enlargement of the electron dephasing rate. This effect crucially depends on the extent, to which electron scatterers, such as boundaries and impurities, are dragged by phonons. Static and vibrating scatterers are described by two dimensionless parameters $q_T l$ and $q_T L$, where $q$ is the wavevector of the thermal phonon, $l$ is the total electron mean-free path, $L$ is the mean-free path due to scattering from static scatterers. According to the Pippard ineffectiveness condition [1], without static scatterers the dephasing rate at low temperatures is slower by the factor $1/ql$ than the rate in a pure bulk material. However, in the presence of static potential the dephasing rate turns out to be $1/qL$ times faster. Thus, at low temperatures electron dephasing and energy relaxation may be controlled by electron boundary/impurity scattering in a wide range.



**Key words:** electron–phonon interaction, dephasing, disorder.

## 1. Introduction

In recent years, the electron dephasing in ultrathin films, nanostructures and mesoscopic devices has been intensively studied. Temperature-dependent dephasing rate is mainly determined by the electron–electron and electron–phonon interactions. While theoretical results pertaining to electron–electron scattering are confirmed by many experiments, the electron–phonon mechanism is still poorly understood. Unfortunately, most researchers employ the standard clean-limit concept, its uncritical application leads to incorrect and controversial conclusions. A reliable electron–phonon interaction model taking into account electron scattering from boundaries, defects and impurities is of vital importance.

If scattering potential of boundaries and impurities is completely dragged by phonons, the inelastic electron scattering from this potential may be excluded by a transformation to the frame, which moves together with the phonon. Using transformation to the local frame, Pippard [1] has found that the electron–phonon coupling depends substantially on the parameter $ql$, where $q$ is the wavevector of the phonon, and $l$ is the electron mean-free path. If $ql < 1$, the electron–phonon coupling is a factor of $1/ql$ weaker than the coupling in the pure limit, $l \to \infty$. This statement is well known as the Pippard ineffectiveness condition [2]. It was confirmed by microscopic calculations in [3, 4].

0749–6036/00/050499 + 06 $35.00/0 

Obviously the Pippard's assumption about completely dragged scatterers is not valid in the presence of rigid boundaries or heavy defects. To generalize Pippard's model we take into account additional static potential. We show that even relatively weak static potential drastically changes the effective electron–phonon coupling and corresponding electron dephasing rate.

## 2. Model

We start with the Hamiltonian, which describes the 'pure' electron–phonon interaction and the interaction between electrons and scatterers that are completely dragged by phonons [3],

$$H_{int} = \sum_{\boldsymbol{p},\boldsymbol{q}} g(\boldsymbol{q}) c^{+}_{\boldsymbol{p}+\boldsymbol{q}} c_{\boldsymbol{p}} (b_{\boldsymbol{q},n} + b^{+}_{-\boldsymbol{q},n}) + \sum_{\boldsymbol{p},\boldsymbol{k},\boldsymbol{R}_\alpha} V(\boldsymbol{k}) c^{+}_{\boldsymbol{p}} c_{\boldsymbol{p}-\boldsymbol{k}} \exp(-i\boldsymbol{k}\boldsymbol{R}_\alpha) + \sum_{\boldsymbol{p},\boldsymbol{k},\boldsymbol{q},\boldsymbol{R}_\alpha} \gamma(\boldsymbol{k},\boldsymbol{q}) c^{+}_{\boldsymbol{p}} c_{\boldsymbol{p}-\boldsymbol{k}} (b_{\boldsymbol{q},n} + b^{+}_{-\boldsymbol{q},n}) \exp[-i(\boldsymbol{k}-\boldsymbol{q})\boldsymbol{R}_\alpha], \tag{1}$$

where $c^{+}_{\boldsymbol{p}}$ is the electron creation operator, $b^{+}_{\boldsymbol{q},n}$ is the creation operator of a phonon with a wavevector $\boldsymbol{q}$ and polarization index $n$, and $\boldsymbol{R}_\alpha$ are the equilibrium positions of scatterers.

The first term with the vertex $g = (2\epsilon_F/3) \times (\boldsymbol{q}\cdot\boldsymbol{e}_n)/(2\rho\omega)^{1/2}$ ($\epsilon_F$ is the Fermi energy, $\boldsymbol{e}_n$ is the phonon polarization vector, $\rho$ is the density) corresponds to the pure electron–phonon scattering. The second term describes the elastic electron scattering from the potential of boundaries and impurities, $V(k)$. If this potential is completely dragged by phonons, the vertex of inelastic electron scattering is given by [3, 5]: $\gamma(\boldsymbol{k},\boldsymbol{q}) = -iV(\boldsymbol{k}\boldsymbol{e}_n)/(2\rho\omega_q)^{1/2}$.

Now we take into account the static scatterers, such as rigid boundaries and heavy defects. Then the total momentum relaxation rate is $\tau^{-1} = \tau_d^{-1} + \tau_s^{-1}$, where $\tau_d^{-1}$ is the electron momentum relaxation rate due to scatterers that are dragged by phonons, and $\tau_s^{-1}$ is the relaxation rate due to static scatterers. It is convenient to introduce the electron mean-free path, $l = v_F\tau$, and the electron-free path with respect to scattering from static potential, $L = v_F\tau_s$.

## 3. Electron dephasing rate

Calculations employing the Keldysh diagrammatic technique for nonequilibrium processes show that the collision integral, which describes the interaction between longitudinal phonons and electrons in a disordered conductor with static and vibrating scattering potentials, is given by

$$I_{e-l.ph}(\epsilon) = -\frac{2\beta_l}{(p_F u_l)^2} \int d\omega_q\, \omega_q^2 R(\epsilon,\omega_q) \left[ \frac{ql\arctan(ql)}{ql - \arctan(ql)} - \left(1 - \frac{l}{L}\right)\frac{3}{(ql)} \right], \tag{2}$$

where $\zeta_0 = \arctan(ql)/(ql)$, the dimensionless constant of the electron–phonon interaction $\beta_l = (2\epsilon_F/3)^2\nu/2\rho u_l^2$ ($\nu$ is the electron density of states, $u_l$ is the longitudinal sound velocity), and $R(\epsilon,\omega_q)$ is the combination of electron ($n_\epsilon$) and phonon ($N_\omega$) distribution functions: $R(\epsilon,\omega) = N_\omega n_\epsilon(1-n_{\epsilon+\omega}) - (1+N_\omega)(1-n_\epsilon)n_{\epsilon+\omega}$. Then the dephasing/relaxation rate of electrons is given by

$$\frac{1}{\tau_{e-l.ph}(0)} = \frac{7\pi\zeta(3)}{2} \frac{\beta_l T^3}{(p_F u_l)^2} F_l(q_T l), \tag{3}$$

$$F_l(z) = \frac{2}{7\zeta(3)} \int_0^{A_l} dx\; \Phi_l(xz)\,(N_x + n_x)\, x^2, \quad \Phi_l(x) = \frac{2}{\pi}\left[ \frac{x\arctan(x)}{x - \arctan(x)} - \left(1 - \frac{l}{L}\right)\frac{3}{x} \right], \tag{4}$$

where $A_{t(l)} = \theta_D l/u_{t(l)} z$ ($\theta_D$ is the Debye temperature). In the limiting cases the relaxation rate is

$$\frac{1}{\tau_{e-l.ph}(0)} = \frac{7\pi\zeta(3)}{2} \frac{\beta_l T^3}{(p_F u_l)^2} \times \begin{cases} 1, & Tl > u_l, \\ \frac{2\pi^3}{35\zeta(3)}\frac{Tl}{u_l} + \frac{3\pi}{7\zeta(3)}\frac{u_l}{TL}, & Tl < u_l. \end{cases} \tag{5}$$

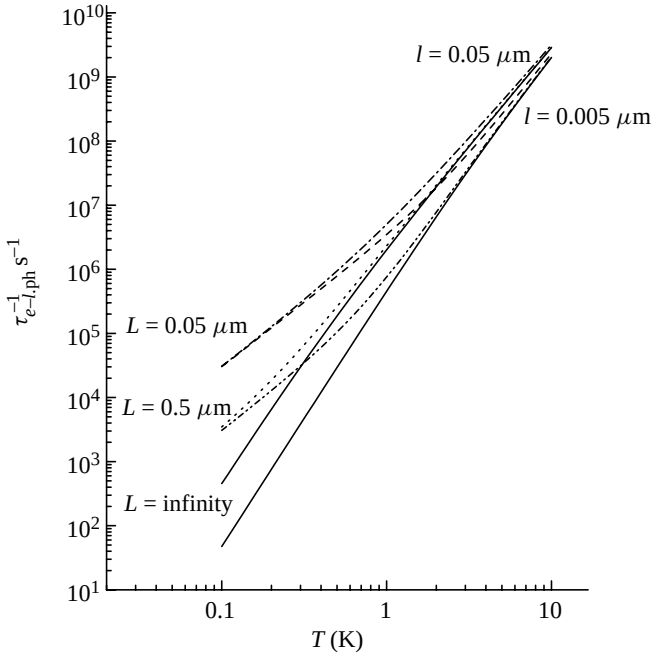


**Fig. 1.** Electron dephasing rate due to longitudinal phonons in Al structures with electron mean-free path $l = 0.005$ $\mu$m and 0.05 $\mu$m. Solid lines correspond to complete drag of all scatterers (boundaries and impurities) by phonons. Dashed and dotted lines correspond to the electron mean-free path with respect to the static potential $L = 0.05$ $\mu$m and 0.5 $\mu$m.

Now we consider interaction of electrons and transverse phonons. The corresponding collision integral has a form

$$I_{e-t.ph}(\epsilon) = -\frac{12\beta_t T^2}{(p_F u_t)(p_F l)}\left(1-\frac{l}{L}\right)\int d\omega_q R(\epsilon,\omega_q)\left[1+\left(1-\frac{l}{L}\right)\frac{3ql-3((ql)^2+1)\arctan(ql)}{2(ql)^3}\right], \quad (6)$$

where the dimensionless constant is $\beta_t = \beta_l(u_l/u_t)^2$, and $u_t$ is the transverse sound velocity. Then the electron dephasing/relaxation rate is given by

$$\frac{1}{\tau_{e-t.ph}(0)} = \frac{3\pi^2\beta_t T^2}{p_F^2 u_t}\left(\frac{1}{l}-\frac{1}{L}\right)F_t(q_T l), \quad (7)$$

$$F_t(z) = \frac{4}{\pi^2}\int_0^{A_t} dx\Phi_t(xz)(N_x + n_x^{eq})x, \quad \Phi_t(x)$$

$$= 1+\left(1-\frac{l}{L}\right)\frac{3x-3(x^2+1)\arctan(x)}{2x^3}. \quad (8)$$

In the limiting cases the electron relaxation rate is

$$\frac{1}{\tau_{e-t.ph}(0)} = \frac{3\pi^2\beta_t T^2}{p_F^2 u_t}\left(\frac{1}{l}-\frac{1}{L}\right)\times\begin{cases}1, & Tl > u_t,\\ \frac{l}{L}+\left(1-\frac{l}{L}\right)\frac{\pi^2}{10}\left(\frac{Tl}{u_t}\right)^2, & Tl < u_t.\end{cases} \quad (9)$$

Therefore, in the impure case ($Tl < u_l, u_t$), the total electron dephasing/relaxation rate is given by

$$\frac{1}{\tau_{e-ph}(0)} = \frac{\pi^4 T^4}{5}(p_F l)\left[\frac{\beta_l}{(p_F u_l)^3}+\frac{3\beta_t}{2(p_F u_t)^3}\left(1-\frac{l}{L}\right)\right]+\frac{3\pi^2 T^2}{2p_F L}\left[\frac{\beta_l}{p_F u_l}+\frac{2\beta_t}{p_F u_t}\left(1-\frac{l}{L}\right)\right]. \quad (10)$$

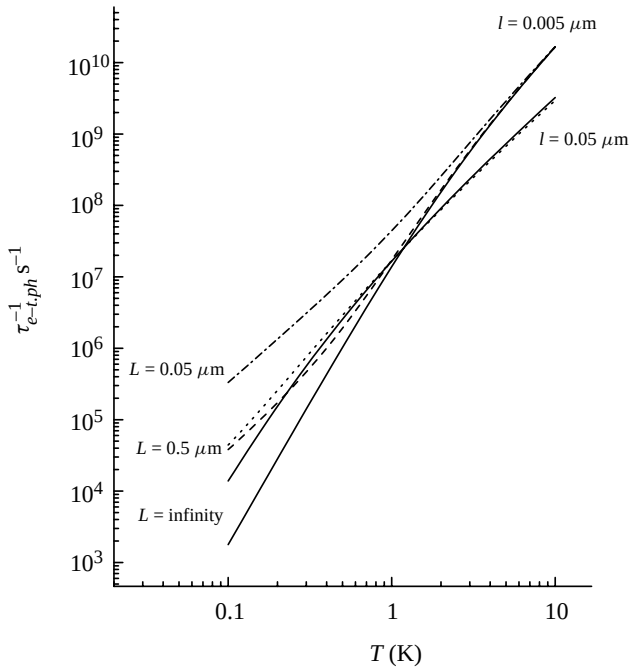


**Fig. 2.** Electron dephasing rate due to transverse phonons in Al structures with electron mean-free path $l = 0.005$ $\mu$m and 0.05 $\mu$m. Solid lines correspond to complete drag of all scatterers (boundaries and impurities) by phonons. Dashed and dotted lines correspond to the electron mean-free path with respect to the static potential $L = 0.05$ $\mu$m and 0.5 $\mu$m.

## 4. Discussion

The presence of static and vibrating electron scatterers leads to complex quantum interference between different scattering mechanisms. If boundaries, defects and impurities are completely dragged by phonons ($L \to \infty$), we reproduce results of Ref. [4] for the electron–phonon dephasing rate. In agreement with the Pippard ineffectiveness condition, at low temperatures the electron–phonon dephasing rate is $u/(Tl)$ times slower than the rate in a pure conductor, $1/\tau_{e-ph} \propto T^4 l$. Note, that in our model with spherical Fermi surface, only longitudinal phonons interact with electrons in the pure conductor. Inelastic electron scattering from boundaries and impurities generates a new channel of the electron–phonon interaction. Due to vibrating boundaries and impurities, transverse phonons can interact with electrons. In the pure limit, $Tl/u \gg 1$, this channel is $Tl/u$ times weaker than the pure electron–phonon coupling. In the dirty limit, $Tl/u \ll 1$, both channels are enhanced due to the diffusion electron motion, in the same way as the electron–electron interaction in impure conductors. However, the quantum interference between these two channels of electron scattering neglects the total effects and results in the Pippard ineffectiveness condition.

This picture is changed in the presence of additional static potential or due to incomplete drag of boundaries and impurities by phonons. In the limit $Tl/u \ll 1$, where the interference is important, the electron dephasing rate turns out to be $u/(TL)$ times faster than the rate in the pure conductor, $1/\tau_{e-ph} \propto T^2/L$. Note, that compared with the dephasing rate due to longitudinal phonons, the contribution of transverse phonons consists of the large factor $(u_l/u_t)^3$ and the factor $(1 - l/L)$. The factor $(1 - l/L)$ has a simple interpretation: it is proportional to the concentration of vibrating scatterers, which provide the interaction between electrons and transverse phonons. If this factor is not too small, the effect of transverse phonons dominates at low temperatures. Note, that the $T^2/l$-term in the relaxation rate due to vibrating impurities

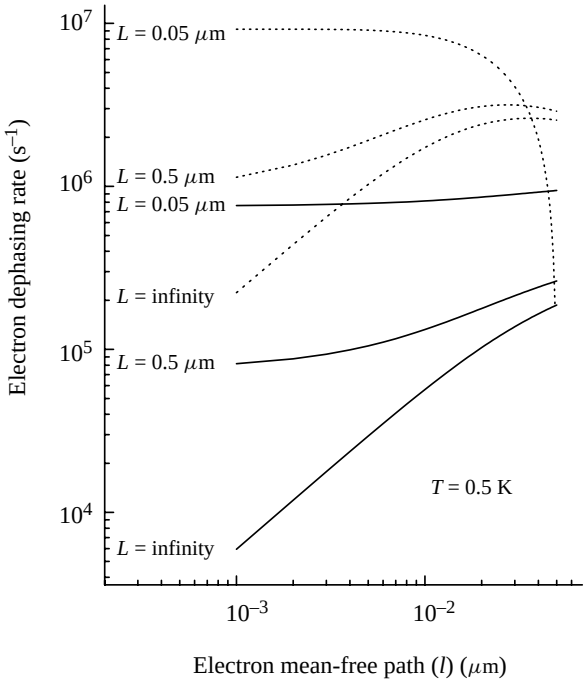


**Fig. 3.** Dependence of the dephasing rate on the electron mean-free path. Solid and dotted lines represent contributions of longitudinal and transverse phonons, correspondingly.

has been obtained by many authors [6]. This result is wrong and contradicts to the Pippard ineffectiveness concept. Only in the presence of the static potential do we obtain a $T^2$-term proportional to $1/L$.

To illustrate our results, we calculate the electron dephasing rate in Al structures with $u_l = 6.3 \times 10^5$ cm s$^{-1}$, $u_t = 3.1 \times 10^5$ cm s$^{-1}$, $v_F = 1.3 \times 10^8$ cm s$^{-1}$, $\beta_l = 1.14$, and $\beta_t = 4.7$ [5]. Temperature dependencies of the dephasing rate in the structures with the electron mean-free path 0.05 $\mu$m and 0.005 $\mu$m are presented in Figs 1 and 2. Solid lines show the dephasing rate under the Pippard ineffectiveness condition. At low temperatures the dephasing becomes faster in the presence of the static potential. Comparing Figs 1 and 2, we see that at low temperatures the electron dephasing is determined by transverse phonons. Figure 3 shows the dependence of the dephasing rate on the electron mean-free path. In the case of complete drag of boundaries and defects, the dephasing rate is proportional to $l$ at low temperatures. In the presence of the static potential, the relaxation rate is determined mainly by the electron mean-free path with respect to scattering from the static potential.

It is important for applications, that the electron–phonon dephasing rate in mesoscopic devices may be changed in a wide range. It can be increased or decreased compared to the rate in a pure bulk material. Some experimental data support our conclusions. The enhancement of the electron–phonon interaction due to disorder has been found in thin metallic films [7] and semiconducting heterostructures [8]. The $T^2$-dependence of the electron–phonon dephasing rate is widely observed in experiments [9]. Some important points, such as the modification of the phonon spectrum, deserve further theoretical investigations.

*Acknowledgement*—This work was supported by the US ARO.

## References

[1] A. B. Pippard, Phil. Mag. **46**, 1104 (1955).
[2] J. M. Ziman, *Electrons and Phonons* (Clarendon, Oxford, 1960) p. 213.
[3] G. Grünvald and K. Scharnberg, Z. Phys. **268**, 197 (1974).
[4] J. Rammer and A. Schmid, Phys. Rev. **B34**, 1352 (1986).
[5] M. Yu. Reizer and A. V. Sergeev, Zh. Exsp. Teor. Fiz. **92**, 2291 (1987); [Sov. Phys. JETP **65**, 1291 (1987)]; N. G. Ptitsina*et al*., Phys. Rev. **B56**, 10089 (1997).
[6] G. Bergman, Phys. Rev. **B3**, 3797 (1971); H. Takayama, Z. Phys. **263**, 329 (1973); S. G. Lisitsin, Sov. J. Low Temp. Phys. **1**, 728 (1975); S. J. Poon and T. H. Geballe, Phys. Rev. **233**, (1978).
[7] J. J. Lin and C. Y. Wu, Europhys. Lett. **29**, 141 (1995).
[8] A. Mittal, R. G. Wheeler, M. W. Keller, D. E. Prober, and R. N. Sacks, Surf. Sci. **361–362**, 537 (1996).
[9] G. Bergmann, Phys. Rep. **107**, 1 (1984).